Optical and magnetic properties of bulk Cobalt and Cobalt clusters.

Maria Pogodaeva

March 29, 2021

Contents

1 Introduction

Comprehensive studies of Cobalt properties have been started in the 1970s. Specifically, in 1974 there was published a paper [1], describing conductivity $\sigma(E)$ of bulk Cobalt as a function of an incident photon energy. The shape of real and imaginary parts of this function are represented on figure fig:jc.

Optical conductivity and dielectric function are connected with the following formula:

$$\sigma_{ext} = 9\frac{\omega \varepsilon_m^{1/2}}{c} V \frac{\varepsilon_m \varepsilon_2(\omega)}{\left[\varepsilon_1(\omega) + 2\varepsilon_m\right]^2 + \varepsilon_2^2(\omega)} \quad (1)$$

Figure 1: Cobalt conductivity

Thus, if the conductivity of the material is known, one can easily derive its absorption spectrum $A(\omega)$, since it is connected to the dielectric function $A(\omega) = Im(\varepsilon(\omega)) = \varepsilon_2(\omega)$. The absorption spectrum of Cobalt was derived from the data on the fig.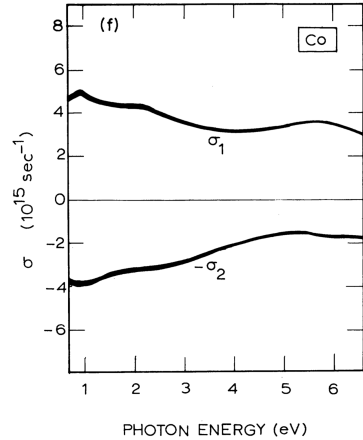 fig:jc using formula sigma and plotted on the fig. fig:drachev with the black colour. Also, absorption spectrum of Cobalt clusters was measured experimentally and also plotted on the same figure with the red colour. The first data indeed is direct measurement of absorption, while the second one implies theoretical background. One can see a serious inconsistency between these two graphs, both of which are derived from experiment. It might happen because formula sigma ignores spin. The global goal of my Skoltech PhD program is to find the reason of such a behavior.
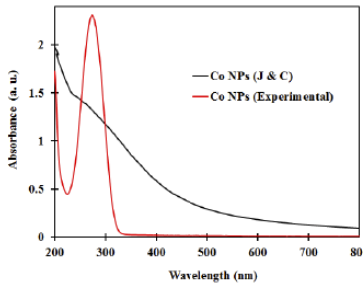
Also, in paper [2] it was mentioned that for ensemble of clusters the magnetization per atom is $0.7\mu_B$, while for bulk hcp and fcc Cobalt it is around $1.7\mu_B$.

Thus, the **goal** of my course project is to:

1) find the dielectric function of both hcp and fcc bulk Cobalt;

2) construct hcp and fcc Cobalt clusters, relax them and calculate their magnetic moment.

Figure 2: Absorption spectrum of Cobalt nanoparticles

2 Methods

For bulk structures it is convenient to use software which implies plane-wave basis sets because of periodicity reasons. For clusters is it better to use atomic-orbitals basis software because of the absence of periodicity in cluster. It does not mean that we are obliged to do so, however, this might simplify and speed up calculations.

Thus, for bulk *hcp* and *fcc* Cobalt **ABINIT** [3] will be used. The following steps should be done:

1) checking how the convergence of lattice constant and magnetic moment depends on the:
- energy cutoff
- k-point mesh
- temperature smearing

2) checking how U_{eff} improves converged values for DFT+U

3) DOS visualization

4) Dielectric function visualization both for majority and minority carriers.

For the cluster calculations there will be used **FHI-aims** [4]. The work will include calculations for both fcc and hcp clusters:

1) Wulff construction

2) Clusters relaxation

3) Calculation of DOS and magnetic moment of clusters.

3 Bulk

3.1 FCC

3.1.1 ECUT convergence

In this calculation I ran convergence tests for k-point grid **$16 \times 16 \times 16$** and Gaussian smeating = **$0,3eV$**. Later, in the section of k-point convergence we shall see, why so. We started the energy cutoff convergence tests from 12 Ha, because pseudopotential energy cutoff starts with this value. One can see that it converges fastly and 25 Ha is enough to reach convergence.

The results of energy cutoff calculations look like this:

Face-centered cubic Cobalt

Cutoff energy, Ha	Lattice constant, Bohr	Magn moment,μ_B,	Energy, $Ha \cdot 10^2$
12	6.660	1.647	-1.46394
15	6.655	1.647	-1.46398
20	6.657	1.649	-1.46406
25	6.655	1.649	-1.46407
30	6.654	1.649	-1.46408
35	6.655	1.649	-1.46408
40	6.655	1.649	-1.46408
45	6.655	1.649	-1.46408
50	6.655	1.649	-1.46408
Experiment	6.695	1.75	

3.1.2 K-mesh convergence for different tsmear

In the previous section we found out that energy cutoff of 25 Hartree is enough for reaching convergence. Let us now check convergence with respect to k-points (but obviously we have a spoiler from the previous section). For this study we use Gaussian smearing.

Here we check convergence for five different values of tsmear: $0.01eV$, $0.05eV$, $0.1eV$, $0.5eV$, $1.0eV$. We do not plot the convergence of total energy, because it is always converged by k-point value $8 \times 8 \times 8$.

One can see that for 1.0 eV and 0.5 eV the convergence is very fast: for k-point mesh $8 \times 8 \times 8$ both magnetic moment and lattice constant are already converged. However, the fastest does not mean the best. Converged values for 1.0 eV smearing are quite poor: $0.9\mu_B$, while the experimental value is $1.75\mu_B$. The value of 0.5 eV makes convergence much better: it underestimates lattice constant the least of all the rest tsmear, but underestimates magnetic moment the most. Still, the accuracy of DFT-calculated magnetic moment with collinear spin is not very high by itself, so there is only one significant digit after coma and here the difference is not that dramatic: it is $1.6\mu_B$ compared to $1.7\mu_B$ for less smearing.
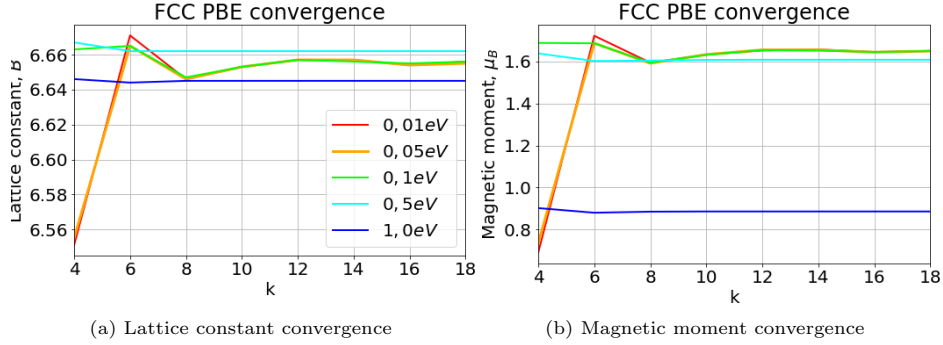
(a) Lattice constant convergence

(b) Magnetic moment convergence

Figure 3: K-point convergence for different tsmear values

3.1.3   DFT+U

One can notice that PBE exchange-correlation functional underestimates lattice constant and magnetic moment compared to experiment. That is why in this section we introduce PBE+U calculation and check convergence of lattice constant and magnetic moment. All calculations in this section were provided with ecut = 30.0 Ha, k-point mesh $16 \times 16 \times 16$ and Gaussian smearing with width $0.01eV$. From PBE we consider these values to be enough

In literature there are rarely reported separately U and J values for Cobalt. There is usually reported U_{eff} and it lies in the range of 2-7 eV. The only separately mentioned $U = 7.8eV$ and $J = 0.92eV$. That is why i started my research from $J = 1.0eV$. One can see that dependence of parameters of U_{eff} is severely non-smooth, with sharp deviations, and practically everywhere DFT+U severely overestimates both lattice constant and magnetic moment.
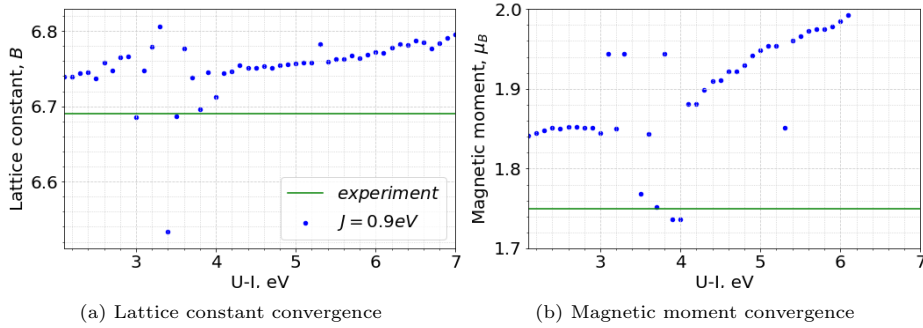

(a) Lattice constant convergence

(b) Magnetic moment convergence

Figure 4: U_{eff} convergence for different tsmear values

5

3.1.4 Density of states

Density of states was calculated at a dense k-point grid $30 \times 30 \times 30$ for fcc and $30 \times 30 \times 30$ and gaussian smearing of 0.2 eV. For DFT+U calculation there were used values $U = 4.0eV$ and $J = 1.0eV$. DOS was compared to the reference DOS from paper [5]. Authors use $20 \times 20 \times 20$ k-point grid, $U_{eff} = 3.0eV$ and Gaussian smearing 0.2 eV. PBE DOS are very similar. PBE+U DOS are a bit different in terms of height and width of the peaks, which might be explained by slightly different J values (they did not report it).
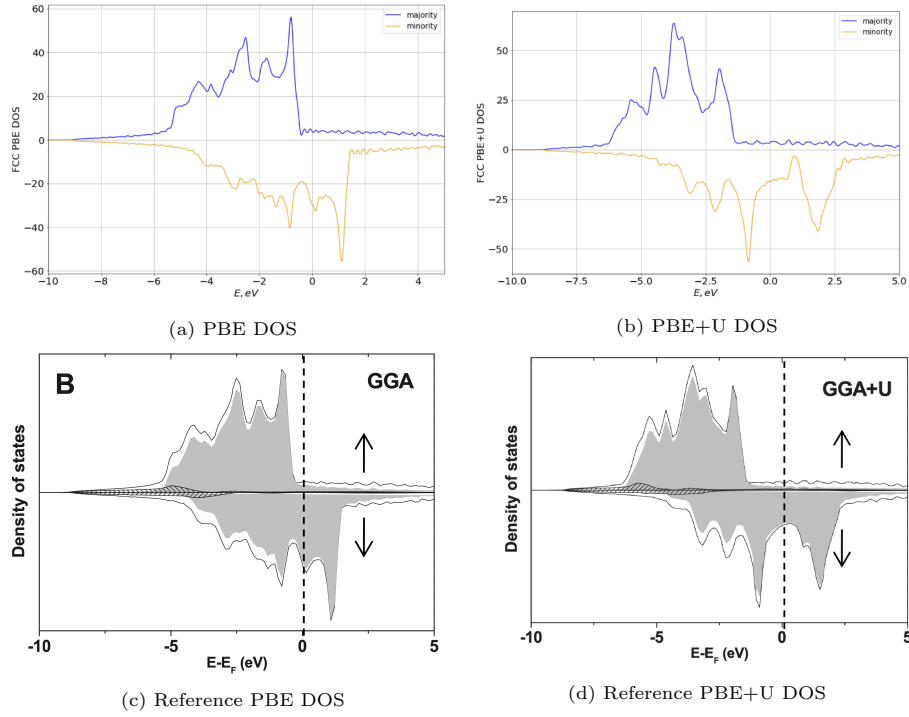

(a) PBE DOS

(b) PBE+U DOS

(c) Reference PBE DOS

(d) Reference PBE+U DOS

Figure 5: FCC DOS and its comparison with reference values

3.1.5 Dielectric function

There are plotted real and imaginary parts of dielectric function for fcc Cobalt relaxed with PBE exchange-correlation functional. One can see almost uniform distribution for majority carriers and jagged plot for minority ones. It is explained by absence of unoccupied states for majority and sharp unoccupied states for minority carriers. Finally, the main contribution into the non-smooth total dielectric function is made by minority carriers, while majority only increase the absolute value of the function, but almost do not affect its shape.
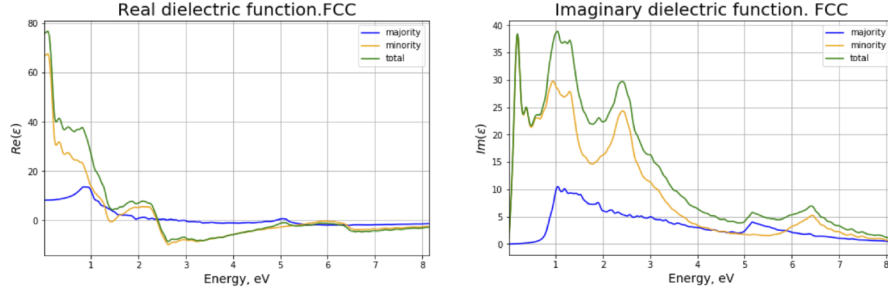
6

Figure 6: Comparison of real and imaginary parts of dielectric function for majority and minority carriers

3.2 HCP

3.2.1 ECUT convergence

Hexagonal Close-Packed Cobalt

Cutoff energy (Ha)	a, Bohr	c, Bohr	Magnetic moment,μ_B,	Total energy, $Ha \cdot 10^2$
12	4.678	7.544	2.0	-2.92779
15	4.675	7.539	2.0	-2.92786
20	4.677	7.541	2.0	-2.92802
25	4.674	7.537	2.0	-2.92805
30	4.674	7.537	2.0	-2.92806
Experiment	4.730	7.667	1.75	

Testing of cutoff energy convergence was conducted at Gaussian smearing 0.1 eV for k-point mesh $18 \times 18 \times 12$. One can see an underestimation of lattice constants and overestimation of magnetic moment. Anyway, this overestimation will be with us in all ABINIT calculations of hcp phase so far.

3.2.2 K-mesh convergence for different tsmear

For different values of tsmear there is a trend of saving overestimated value of magnetic moment and underestimated lattice constants. However, for high tsmear value at some point magnetization drops to zero.

Here I do not plot magnetization, since it remains constant all the way for each and every K-point, unless there is a sharp hop of lattice constant dependence. Magnetization drops to zero at such points:

a) for 0.01 eV - nowhere
b) for 0.05 eV - nowhere
c) for 0.1 eV - at K=12
d) for 0.5 eV - everywhere
e) for 1.0 eV - everywhere

One can see that for tsmear 0.01 eV the convergence is reached very quickly, which might mean that in future we have to try even less tsmear value.
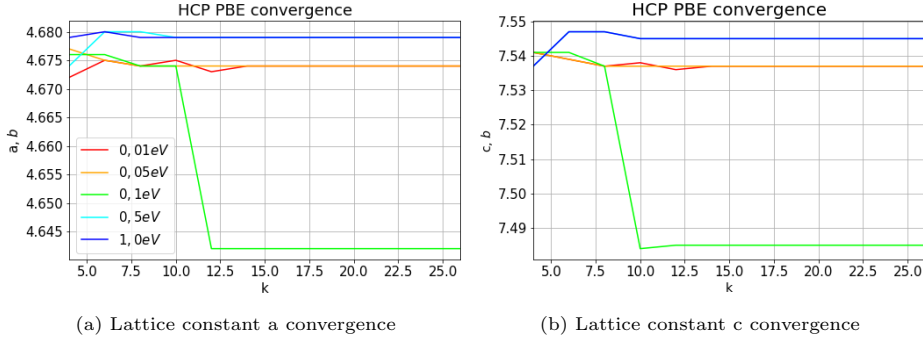
(a) Lattice constant a convergence   (b) Lattice constant c convergence

Figure 7: K-point convergence of lattice parameter for different tsmear values

3.2.3 DFT+U

Opposite to FCC DFT+U dependence, here one can find a very beautiful and smooth dependence of both lattice constants on the U_{eff} parameter. $U_{eff} = 2.6eV$ is the best possible value in terms of coincidence with experiment. However, the main point of introducing U_{eff} was to correct overestimated magnetic moment per atom and resulting unphysical DOS. However, even though in the region around 3 eV there is a slight change of magnetic moment, it is very minor - $1.997\mu_B$. However, my research has shown that increasing J value might affect magnetic moment dramatically: for J=0.85 there are only two value of magnetic moment below 2, while for J=1.0 there are 10 of these values. This is a field of further improvement of my results.

3.2.4 Density of states

Density of states was calculated at a dense k-point grid $30 \times 30 \times 18$ and gaussian smearing of 0.2 eV. For DFT+U calculation there were used values $U = 4.0eV$ and $J = 1.0eV$. DOS was compared to the reference DOS from paper [5]. Authors use $20 \times 20 \times 20$ k-point grid, $U_{eff} = 3.0eV$ and Gaussian smearing 0.2 eV. PBE DOS is very similar. PBE+U DOS is a bit different in terms of height and width of the peaks, which might be explained by slightly different J values (they did not report it). Big difference for both DOS is the drop to exact zero at some point which never happens neither to reference DOS nor for fcc DOS, calculated above.

3.2.5 Dielectric function

T:q here are plotted real and imaginary parts of dielectric function for hcp Cobalt relaxed with PBE exchange-correlation functional. One can see zero distribution for majority carriers and jagged plot for minority ones. Although majority value is unphysical, it coincides well with zero density of states above Fermi level and magnetic moment of μ_B for these carriers. The only cotribution

(a) Lattice constant (a) dependence as a function of U_{eff}

(b) Lattice constant (c) dependence as a function of U_{eff}

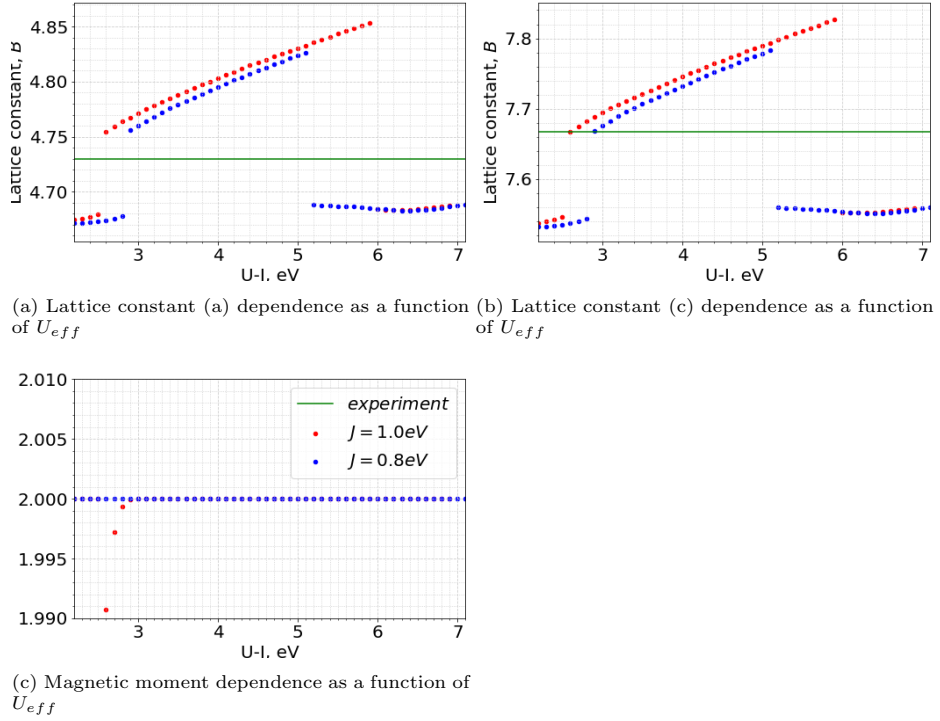(c) Magnetic moment dependence as a function of U_{eff}

Figure 8: Parameters convergence as a function of U_{eff} for different J values

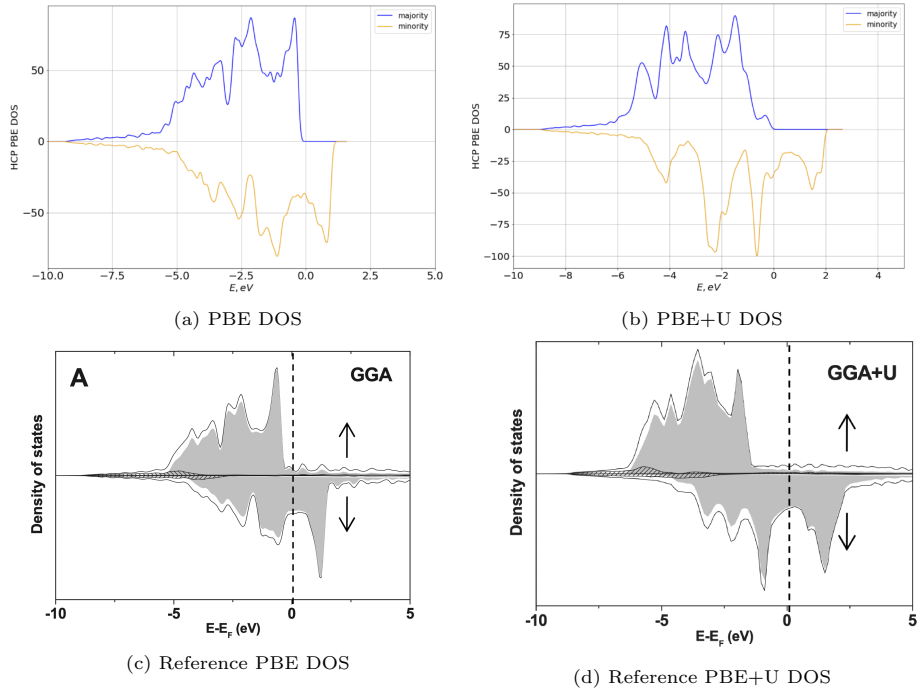into imaginary and real parts of dielectric function comes from minority carriers (and vacuum for real part as well).

9

(a) PBE DOS

(b) PBE+U DOS

(c) Reference PBE DOS

(d) Reference PBE+U DOS

Figure 9: HCP DOS and its comparison with reference values
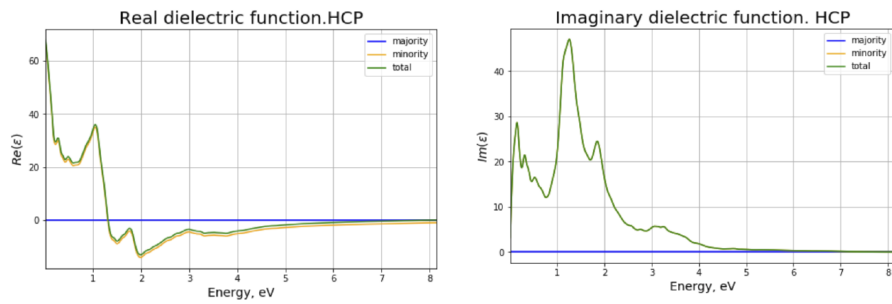
Figure 10: Comparison of real and imaginary parts of dielectric function for majority and minority carriers

4 Clusters

In the experimental study [2] there are reported both hcp and fcc packings inside clusters. Using methods of electron microscopy, authors defined clusters as 'spherical'. The diameter of these clusters is $9nm$, which is approximately 10^4 atoms. Obviously, this limit is far beyond DFT and MD simulations. With DFT we can only model 10^2 atoms. That is why in our simulations we shall consider small particles: ¡ 100 atoms for each packing keeping in mind, that the final result for the particles of another size might differ.

4.1 Wulff construction

While materials are being formed, they tend to minimize their energy. Bulk materials minimize their volume energy, while cluster also have surface energy. The full name of this quantity is Gibbs free energy, and the mathematical expression of this fact is written in the following way:

$$\min_i \Delta G_i = \min \sum_j \gamma_j O_j, \tag{2}$$

where ΔG_i is total surface Gibbs free energy, γ_j is Gibbs free energy of a facet j, and O_j is the area of this facet. The sum is taken over all facets. This way of building clusters is called Wulff construction and was proposed in 1901 by G. Wulff [6].
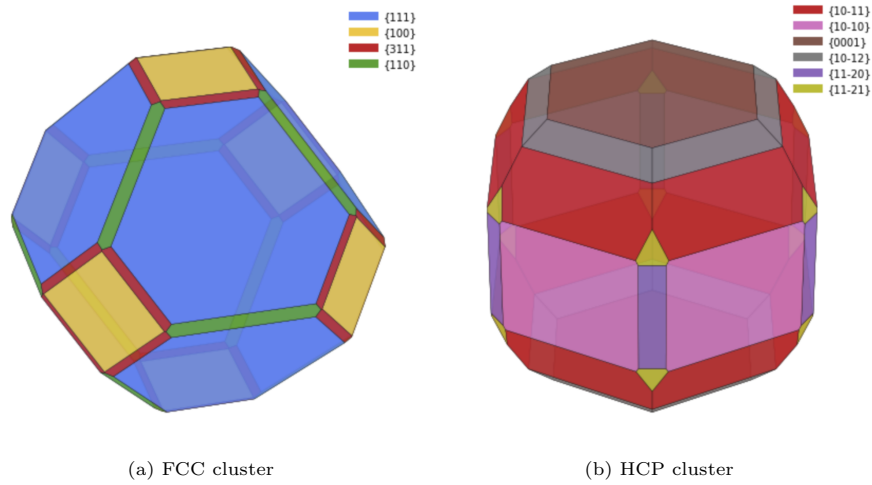

(a) FCC cluster (b) HCP cluster

Figure 11: Wulff constructed Cobalt cluster

In my research I use Gibbs free energies for hcp and fcc Cobalt clusters from the paper [7]. In order to build a cluster I use Python libraries Atomic Simulation Environment aka ASE [8] and WulffPack [9]. The starting point of particles construction was relaxed with PBE bulk geometry for fcc and hcp.

Wulff shapes are represented at figure . The corresponding colors mark Miller planes.
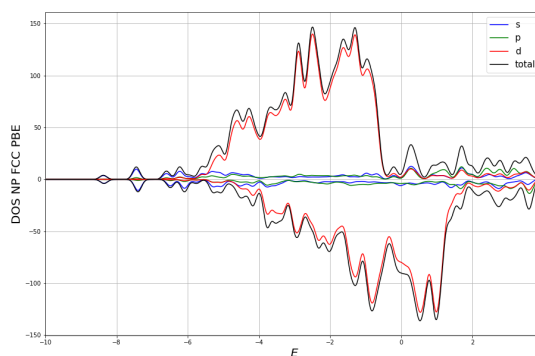
4.2   Relaxed clusters

Wulff constructed hcp nanocluster consists of 48 atoms, while fcc contains 79. The relaxation process leads to the decrease of lattice constant compared to the bulk lattice constant.

packing	a_{bulk}	a_{min}	a_{max}	c_{bulk}	c_{min}	c_{max}
hcp	2.501 A	2.36 A	2.49 A	4.033 A	3.92 A	3.99 A
fcc	3.522 A	3.517	3.33			

4.3   DOS comparison
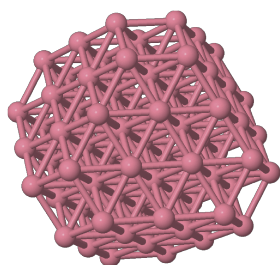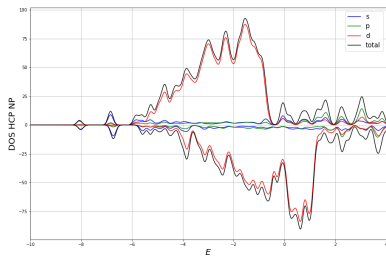

(a) FCC cluster

(b) FCC NP DOS with 79 atoms
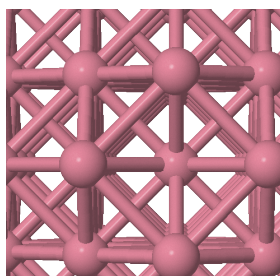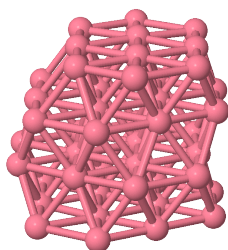

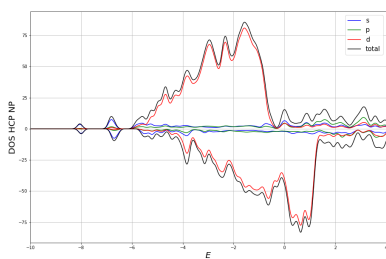(c) FCC bulk
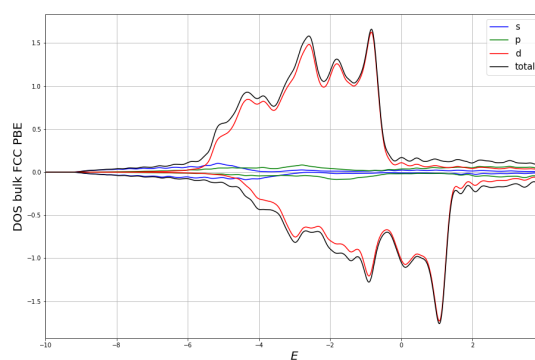
(d) FCC bulk DOS
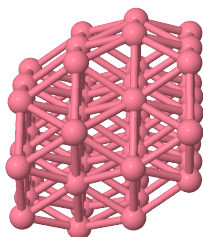
Figure 12: DOS comparison
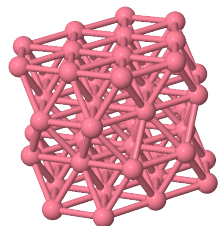
(a) HCP 48 cluster

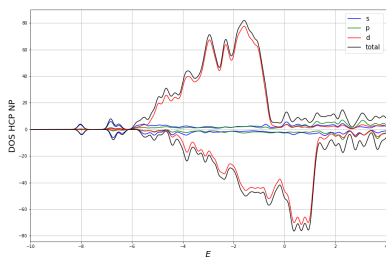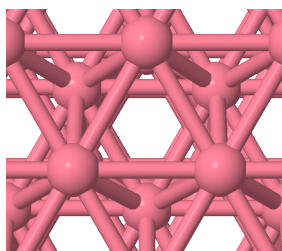(b) HCP NP DOS with 48 atoms

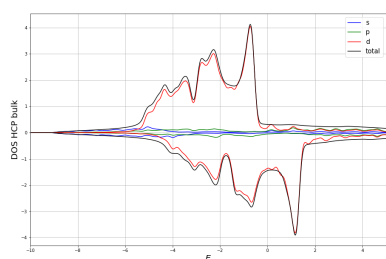(c) HCP 46 cluster

(d) HCP NP DOS with 46 atoms

(e) HCP 44 cluster

(f) HCP NP DOS with 44 atoms

(g) HCP bulk

(h) HCP bulk DOS

Figure 13: DOS comparison

13

References

[1] P. Johnson and R. Christy, "Optical constants of transition metals: Ti, v, cr, mn, fe, co, ni, and pd," *Physical review B*, vol. 9, no. 12, p. 5056, 1974.

[2] H. L. Bhatta, A. E. Aliev, and V. P. Drachev, "New mechanism of plasmons specific for spin-polarized nanoparticles," *Scientific reports*, vol. 9, no. 1, pp. 1–8, 2019.

[3] X. Gonze, B. Amadon, G. Antonius, F. Arnardi, L. Baguet, J.-M. Beuken, J. Bieder, F. Bottin, J. Bouchet, E. Bousquet, N. Brouwer, F. Bruneval, G. Brunin, T. Cavignac, J.-B. Charraud, W. Chen, M. Côté, S. Cottenier, J. Denier, G. Geneste, P. Ghosez, M. Giantomassi, Y. Gillet, O. Gingras, D. R. Hamann, G. Hautier, X. He, N. Helbig, N. Holzwarth, Y. Jia, F. Jollet, W. Lafargue-Dit-Hauret, K. Lejaeghere, M. A. L. Marques, A. Martin, C. Martins, H. P. C. Miranda, F. Naccarato, K. Persson, G. Petretto, V. Planes, Y. Pouillon, S. Prokhorenko, F. Ricci, G.-M. Rignanese, A. H. Romero, M. M. Schmitt, M. Torrent, M. J. van Setten, B. V. Troeye, M. J. Verstraete, G. Zérah, and J. W. Zwanziger, "The abinit project: Impact, environment and recent developments," *Comput. Phys. Commun.*, vol. 248, p. 107042, 2020.

[4] V. Blum, R. Gehrke, F. Hanke, P. Havu, V. Havu, X. Ren, K. Reuter, and M. Scheffler, "Ab initio molecular simulations with numeric atom-centered orbitals," *Computer Physics Communications*, vol. 180, no. 11, pp. 2175–2196, 2009.

[5] V. A. de la Peña O'Shea, I. d. P. Moreira, A. Roldán, and F. Illas, "Electronic and magnetic structure of bulk cobalt: The α, β, and ε-phases from density functional theory calculations," *The Journal of Chemical Physics*, vol. 133, no. 2, p. 024701, 2010.

[6] G. Wulff, "Zur frage der geschwindigkeit des wachstums und der aufliisung der kristallfllchen," *Z. Krist. Miner*, vol. 34, pp. 499–530, 1901.

[7] J.-X. Liu, H.-Y. Su, D.-P. Sun, B.-Y. Zhang, and W.-X. Li, "Crystallographic dependence of co activation on cobalt catalysts: Hcp versus fcc," *Journal of the American Chemical Society*, vol. 135, no. 44, pp. 16284–16287, 2013.

[8] A. H. Larsen, J. J. Mortensen, J. Blomqvist, I. E. Castelli, R. Christensen, M. Dułak, J. Friis, M. N. Groves, B. Hammer, C. Hargus, *et al.*, "The atomic simulation environment—a python library for working with atoms," *Journal of Physics: Condensed Matter*, vol. 29, no. 27, p. 273002, 2017.

[9] J. Rahm and P. Erhart, "Wulffpack: A python package for wulff constructions," *Journal of Open Source Software*, vol. 5, no. 45, p. 1944, 2020.